Comparative Study of Several Time-Domain Methods for Optical Waveguide Analyses

MURAKI, Mitsunori / NAKANO, Hisamatsu / YAMAUCHI, Junji / SHIBAYAMA, Jun

(出版者 / Publisher)
IEEE
(雑誌名 / Journal or Publication Title)
Journal of lightwave technology / Journal of lightwave technology
(号 / Number)
7
(開始ページ / Start Page)
2285
(終了ページ / End Page)
2293
(発行年 / Year)
2005-07

Comparative Study of Several Time-Domain Methods for Optical Waveguide Analyses

Jun Shibayama, *Member, IEEE*, *Member, OSA*, Mitsunori Muraki, Junji Yamauchi, *Member, IEEE*, *Member, OSA*, and Hisamatsu Nakano, *Fellow, IEEE*

***Abstract*—The performance of the recently developed time-domain beam-propagation methods (TD-BPMs) is compared with that of the finite-difference time-domain (FDTD) method. For the TD-BPMs, we investigate full-band (FB), wide-band (WB), and narrow-band (NB) methods based on the implicit finite-difference (FD) schemes. Owing to the use of the slowly varying envelope, a time step of the TD-BPM can be chosen to be larger than that of the FDTD. Although the numerical results of a waveguide grating obtained from the FB- and WB-TD-BPMs agree well with that from the FDTD, the CPU times are longer than that of the FDTD due to the solution of broadly banded matrices. Introducing the alternating-direction implicit method (ADIM) into the WB- and NB-TD-BPMs contributes to a reduction in the CPU time. To make the methods more efficient, a fourth-order accurate FD formula is applied to the ADIM-based WB- and NB-TD-BPMs, leading to reduced CPU times to 40% and 6% of that of the FDTD, respectively.**

***Index Terms*—Beam-propagation method (BPM), finite-difference time-domain method (FDTD), numerical dispersion, time-domain analysis, waveguide grating.**

I. Introduction

THE finite-difference time-domain (FDTD) method [1] is one of the most powerful numerical techniques for the analyses of optical waveguides [2]–[4] and photonic crystals [5]–[7]. The FDTD can grasp all aspects of the optical behavior by virtue of direct discretization of Maxwell's equations. For the FDTD, three spatial components are required to analyze a two-dimensional (2-D) optical waveguide. Because most practical optical waveguides are weakly guiding, scalar or semivector (SV) analysis is often sufficient for many applications. Therefore, the scalar [3] and SV [4] FDTDs have been proposed, where only a single transverse component is calculated. Note that the FDTDs based on the explicit scheme require a small time step to fulfill the stability criterion.

To alleviate the stability criterion, much attention has been paid to the time-domain beam-propagation method (TD-BPM) [8]–[21]. The TD-BPMs developed so far can roughly be divided into three classes, i.e., full-band (FB) [10], [19]–[21], wide-band (WB) [16]–[18], and narrow-band (NB) [8]–[15] TD-BPMs. The feature of the TD-BPM is that only the time-varying optical envelope is analyzed. This allows us to use a larger time step with the implicit scheme than that in the FDTD. However, the usefulness of the TD-BPM has not yet been fully examined.

The purpose of this paper is to investigate the performance of the TD-BPMs, in comparison with the FDTD. To do so, we newly develop FB- and WB-TD-BPMs based on the implicit FD scheme. We also propose a WB-TD-BPM based on the alternating-direction implicit method (ADIM) with an iteration procedure. After presenting the brief formulation of each TD method, we study the numerical dispersion for a one-dimensional (1-D) model. The computational accuracy and efficiency are assessed through analyzing the spectral response of the reflection coefficient for a waveguide grating. Numerical results show that the responses obtained from the FB- and WB-TD-BPMs agree well with that from the FDTD. However, the CPU times are much longer than that of the FDTD due to the solution of broadly banded matrices. It is found that the application of the ADIM to the WB- and NB-TD-BPMs contributes to a reduction in the CPU time.

To further reduce the CPU time of the TD-BPM while maintaining its accuracy, we finally apply a fourth-order accurate FD formula to the ADIM-based TD-BPMs, in which the total number of sampling points is significantly reduced. It is demonstrated that the CPU times of the WB- and NB-TD-BPMs are successfully reduced to 40% and 6% of that of the FDTD, respectively.

II. Time-Domain Methods

A. FDTD Methods

The FDTD is formulated by direct discretization of Maxwell's equations, in which three spatial components are required for the analysis of a 2-D waveguide [2]. For a weakly guiding waveguide, the scalar and SV-FDTDs [3], [4] have been proposed, where only a single transverse component is calculated. For the SV-FDTD, the following wave equation is solved in the time domain:

$$\frac{n^2}{c^2}\frac{\partial^2 \tilde{\phi}}{\partial t^2} = \left(\nabla_x^2 + \nabla_z^2\right)\tilde{\phi} \tag{1}$$

Manuscript received October 19, 2004; revised March 15, 2005. This work was supported in part by the "University-Industry Joint Research" Project for Private Universities: matching fund subsidy from MEXT, 2003–2007.

The authors are with the Faculty of Engineering, Hosei University, Tokyo 184-8584, Japan.

Digital Object Identifier 10.1109/JLT.2005.850032

where

$$\nabla_\alpha^2 = \frac{\partial^2}{\partial \alpha^2}, \quad \tilde{\phi} = \tilde{E}_y \quad \text{(for TE mode)}$$
$$\nabla_\alpha^2 = n^2 \frac{\partial}{\partial \alpha}\left(\frac{1}{n^2}\frac{\partial}{\partial \alpha}\right), \quad \tilde{\phi} = \tilde{H}_y \quad \text{(for TM mode)}$$

in which n and c are the refractive index and the speed of light in a vacuum, respectively, and $\alpha = x$ or z. Unless otherwise noted, we approximate ∇_α^2 using an improved FD formula with second-order accuracy (IFD2) [22], [23]. The temporal second derivative is discretized by the following central difference:

$$\frac{\partial^2 \tilde{\phi}}{\partial t^2} \simeq \frac{\tilde{\phi}^{l+1} - 2\tilde{\phi}^l + \tilde{\phi}^{l-1}}{\Delta t^2}$$

where l indicates the position along the time axis. The resultant FD equation is solved explicitly. It should be noted that the stability criterion still remains.

B. TD-BPMs

In the TD-BPMs, we analytically differentiate the fast carrier component of the optical field and numerically treat only the slowly varying envelope (SVE). Applying the time dependence $\tilde{\phi} = \phi \exp(j\omega_0 t)$, where ϕ is the SVE function and ω_0 is the center carrier frequency, to (1), we have the following FB-TD-BPM equation (although the FB-TD-BPM based on the finite-element scheme has already been developed [19], [20], an FD-based method is newly developed here):

$$\frac{n^2}{c^2}\frac{\partial^2 \phi}{\partial t^2} + \frac{2j\omega_0 n^2}{c^2}\frac{\partial \phi}{\partial t} = \left[\left(\nabla_x^2 + \nabla_z^2\right) + \frac{\omega_0^2 n^2}{c^2}\right]\phi. \quad (2)$$

The temporal second derivative in (2) is discretized by the same central difference as that shown above. The first derivative is discretized as

$$\frac{\partial \phi}{\partial t} \simeq \frac{\phi^{l+1} - \phi^{l-1}}{2\Delta t}.$$

ϕ in the right-hand side of (2) is averaged by

$$\phi \simeq \frac{\phi^{l+1} + \phi^{l-1}}{2}$$

leading to an implicit scheme, in which a large Δt can be used. This formulation corresponds to the Newmark-β scheme with $\beta = 0.5$ [24]. As a result, linear equations are obtained, in which each equation involves five unknowns. Therefore, the system becomes a broadly banded matrix, which can be solved by iteration techniques such as the Bi-CGSTAB [25]. At the first calculation step, we require ϕ^1 and ϕ^0 to obtain ϕ^2. Hence, we calculate ϕ^1 from the given initial field ϕ^0 using the following NB-TD-BPM.

For the NB-TD-BPM, the temporal second derivative in (2) is omitted on the basis of the SVE approximation (SVEA). This results in

$$\frac{\partial \phi}{\partial t} = \left[\zeta\left(\nabla_x^2 + \nabla_z^2\right) + \xi\right]\phi \quad (3)$$

where $\zeta = -jc^2/(2\omega_0 n^2)$ and $\xi = -j\omega_0/2$. Equation (3) forms a parabolic-type equation so that the efficient BPM solvers developed so far can directly be applied to the solution of (3). We solve (3) by the Crank–Nicolson (CN) scheme with and without the ADIM [13], [15]. With the ADIM, the resultant FD equations are efficiently solved by the Thomas algorithm.

To perform a WB analysis without a significant increase in the computational resources, the Padé (1,1) approximant is applied to (2), in which the effect of the temporal second derivative is partially included [16]–[18]. Although the Padé approximant is used for the FD-based TD-BPM in [17], only a 1-D model is treated. Here we treat a 2-D model. The basic equation of the WB-TD-BPM is expressed as

$$\frac{\partial \phi}{\partial t} = \frac{\zeta\left(\nabla_x^2 + \nabla_z^2\right) + \xi}{1 - \frac{j}{2\omega_0}\left[\zeta\left(\nabla_x^2 + \nabla_z^2\right) + \xi\right]}\phi. \quad (4)$$

We apply the CN scheme to (4) and solve the resultant broadly banded matrix by the Bi-CGSTAB.

We also propose a WB-TD-BPM based on the ADIM with an iteration procedure, which is described in the following. Applying the CN scheme to (4), we have

$$\left\{1 - \left(\frac{j}{2\omega_0} + \frac{\Delta t}{2}\right)\left[\zeta\left(\nabla_x^2 + \nabla_z^2\right) + \xi\right]\right\}\phi^{l+1} = \left\{1 - \left(\frac{j}{2\omega_0} - \frac{\Delta t}{2}\right)\left[\zeta\left(\nabla_x^2 + \nabla_z^2\right) + \xi\right]\right\}\phi^l. \quad (5)$$

Note that splitting (5) by the well-known Peaceman–Rachford ADIM [26] gives rise to zeroth-order accuracy. To avoid this, we resort to the Douglas–Rachford-type ADIM [27].

First, we rewrite (5) as

$$\left\{1 - \frac{\Delta t}{2}\left[\zeta\left(\nabla_x^2 + \nabla_z^2\right) + \xi\right]\right\}\phi^{l+1} = \left\{1 + \frac{\Delta t}{2}\left[\zeta\left(\nabla_x^2 + \nabla_z^2\right) + \xi\right]\right\}\phi^l + \frac{j}{2\omega_0}\left[\zeta\left(\nabla_x^2 + \nabla_z^2\right) + \xi\right](\phi^{l+1} - \phi^l). \quad (6)$$

Here we apply the Douglas–Rachford-type ADIM to (6), leading to

$$\left[1-\frac{\Delta t}{2}\left(\zeta\nabla_x^2+\frac{\xi}{2}\right)\right]\times\left\{\left[1-\frac{\Delta t}{2}\left(\zeta\nabla_z^2+\frac{\xi}{2}\right)\right]\phi^{l+1}+\frac{\Delta t}{2}\left(\zeta\nabla_z^2+\frac{\xi}{2}\right)\phi^{l}\right\}=\left[1+\frac{\Delta t}{2}\left(\zeta\nabla_x^2+\frac{\xi}{2}\right)+\Delta t\left(\zeta\nabla_z^2+\frac{\xi}{2}\right)\right]\phi^{l}+\frac{j}{2\omega_0}\left[\zeta\left(\nabla_x^2+\nabla_z^2\right)+\xi\right](\phi^{l+1}-\phi^{l}). \tag{7}$$

We replace the second bracket in the left-hand side of (7) with an intermediate value ϕ^*. As a result, the following two-step algorithm is derived:

$$\left[1-\frac{\Delta t}{2}\left(\zeta\nabla_x^2+\frac{\xi}{2}\right)\right]\phi^{*}=\left[1+\frac{\Delta t}{2}\left(\zeta\nabla_x^2+\frac{\xi}{2}\right)+\Delta t\left(\zeta\nabla_z^2+\frac{\xi}{2}\right)\right]\phi^{l}+\frac{c^2}{4\omega_0^2n^2}\left(\nabla_x^2+\nabla_z^2+\frac{\omega_0^2n^2}{c^2}\right)(\phi^{l+1,m}-\phi^{l}) \tag{8}$$

$$\left[1-\frac{\Delta t}{2}\left(\zeta\nabla_z^2+\frac{\xi}{2}\right)\right]\phi^{l+1,m+1}=\phi^{*}-\left[\frac{\Delta t}{2}\left(\zeta\nabla_z^2+\frac{\xi}{2}\right)\right]\phi^{l} \tag{9}$$

where m indicates the number of iterations. It is worth mentioning that (8) and (9) maintain tridiagonal matrices, which can efficiently be solved by the Thomas algorithm.

Notice that the second term (Padé term) in the right-hand side of (8) contains an unknown value of $\phi^{l+1,m}$ (if the Padé term is omitted, (8) and (9) are equivalent to the equations of the NB-TD-BPM). To take into account the Padé term, we iteratively solve (8) and (9), starting with $\phi^{l+1,1}=\phi^{l}$, until the sequence of $\phi^{l+1,2\cdots m}$ converges (this iteration procedure is similar to that described in [28]). In the practical calculation, we set the convergence criterion to be $\max\left[|\phi^{l+1,m+1}-\phi^{l+1,m}|\right]<10^{-2}$, which is small enough to provide a converged solution of the reflection coefficient in the following analysis.

Note that the constraint on Δt in terms of accuracy is significantly relaxed owing to the use of the SVE, since the fast carrier component is analytically treated. To take full advantage of the SVE, the second-order implicit scheme is favorable for the discretization of the temporal derivatives, considering that a large Δt can be utilized without degrading the accuracy. In the literatures [10], [21], however, the explicit scheme is used to discretize the temporal derivatives, in spite of the use of the SVE. It follows that a small Δt is required to meet the stability criterion, as in the case of the FDTD. This cannot fully exploit the advantage of using the SVE. Therefore, this paper does not treat the TD-BPMs using the explicit scheme.

C. Other TD Methods

Very recently, some other TD methods have been developed, which are closely related to the aforementioned FDTDs and TD-BPMs. For example, the ADIM has been applied to the FDTD based on the SVE [29] and the scalar FDTD [30] for efficient TD analysis. In addition, a combination of the TD-BPM and the reflection method has been investigated [31]. A comparison with these methods, however, is beyond the scope of this paper and will be left for a future study.

III. Numerical Dispersion Analysis

We now study the numerical dispersion of each TD method. Because forward and backward waves traveling in the $\pm z$ directions predominate the properties of the waveguide, we only discuss the 1-D model in the z direction.

The numerical dispersion relation is obtained by substituting a plane wave as [1], [17]

$$\phi=\mathrm{e}^{j(\omega p\Delta t-k_z q\Delta z)} \tag{10}$$

where p and q are the temporal and spatial indices, respectively, into the FD equation. Here we consider second-order FD discretizations in both time and space, in accordance with the formulations done in Sections II-A and II-B.

For the FDTD, the numerical dispersion relation is as follows:

$$\sin\left(\frac{\omega\Delta t}{2}\right)=\frac{c\Delta t}{n\Delta z}\left[\sin\left(\frac{k_z\Delta z}{2}\right)\right]. \tag{11}$$

For the SV-FDTD, the dispersion relation is expressed as

$$\cos(\omega\Delta t)=\left(\frac{c\Delta t}{n\Delta z}\right)^2\left[\cos(k_z\Delta z)-1\right]+1. \tag{12}$$

We have the following dispersion relations:

$$\cos(\omega\Delta t)-\omega_0\Delta t\sin(\omega\Delta t)=\cos(\omega\Delta t)\times\left\{\left(\frac{c\Delta t}{n\Delta z}\right)^2\left[\cos(k_z\Delta z)-1\right]+\frac{(\omega_0\Delta t)^2}{2}\right\}+1 \tag{13}$$

for the FB-TD-BPM

$$\omega=\frac{1}{j\Delta t}\ln\frac{1-\eta\left(\frac{\Delta t}{2}-\frac{j}{2\omega_0}\right)}{1+\eta\left(\frac{\Delta t}{2}+\frac{j}{2\omega_0}\right)} \tag{14}$$

for the WB-TD-BPM, and

$$\omega=\frac{1}{j\Delta t}\ln\frac{1-\eta\frac{\Delta t}{2}}{1+\eta\frac{\Delta t}{2}} \tag{15}$$

for the NB-TD-BPM, where $\eta=4\zeta/\Delta z^2\sin^2(k_z\Delta z/2)-\xi$.

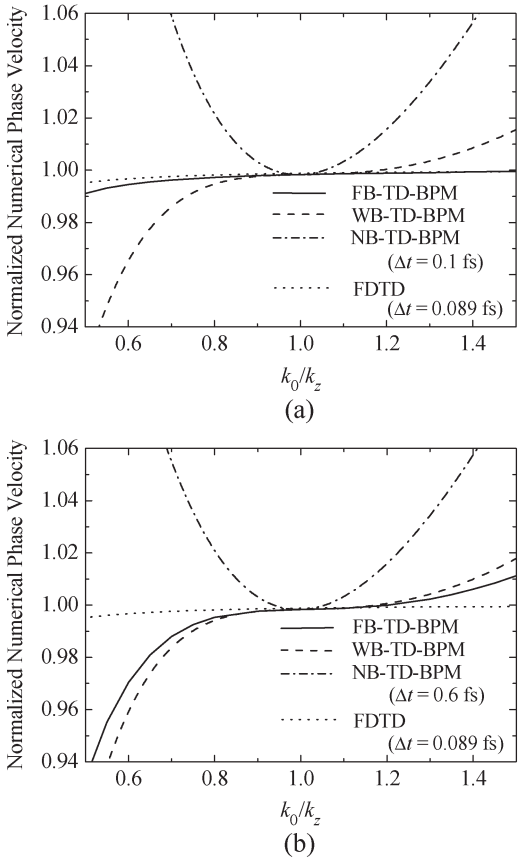

Fig. 1. Normalized numerical phase velocity. For the TD-BPMs, (a) $\Delta t = 0.1$ fs and (b) $\Delta t = 0.6$ fs.

Fig. 1 shows the normalized numerical phase velocity given by $\omega/(k_z c/n)$ for the FDTDs and by $(\omega+\omega_0)/(k_z c/n)$ for the TD-BPMs, where $k_z = 2\pi n/\lambda$. In this calculation, the refractive index n is chosen to be $\simeq 1.21$, which corresponds to the effective index of the TE mode at 1.5 μm for the slab waveguide (without gratings) to be treated in Fig. 2. Δt is chosen to be 0.089 fs for the FDTDs, and 0.1 fs in Fig. 1(a) and 0.6 fs in Fig. 1(b) for the TD-BPMs. Δz is fixed to be 0.04 μm. The numerical parameters used in Fig. 1(b) are consistent with those adopted for the grating analysis in Section IV.

It is seen in Fig. 1 that the phase velocity is almost flat and unity for the FDTD. Although not illustrated, the phase velocity of the SV-FDTD perfectly follows that of the FDTD. For the FB-TD-BPM, the use of $\Delta t = 0.1$ fs significantly improves the property of the phase velocity, when compared with $\Delta t = 0.6$ fs. In contrast, phase velocities of the WB- and NB-TD-BPMs are not sensitive to the choice of Δt. It follows that the ranges of accurate phase velocities are inherently limited for the WB- and NB-TD-BPMs. Nevertheless, the deviations in the phase velocities for $\Delta t = 0.6$ fs [Fig. 1(b)] are kept within $\pm 1\%$ for $0.74 < k_0/k_z < 1.4$ in the former and for $0.85 < k_0/k_z < 1.16$ in the latter. These observations are important when calculating the spectral response of the waveguide grating. In Section IV-A, we will examine how the error in the phase velocity affects the numerical results of the spectral response.

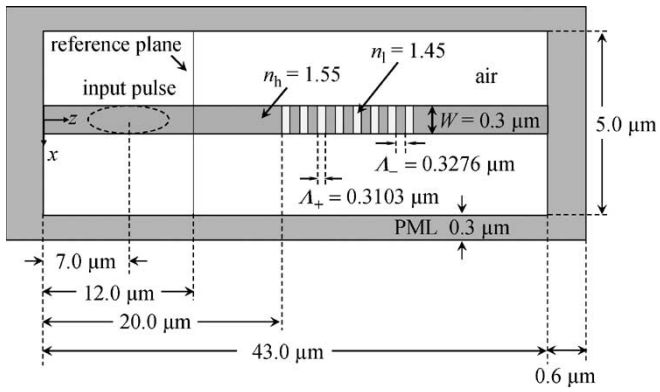

Fig. 2. Configuration of a waveguide grating.

IV. Analysis of Waveguide Grating

Fig. 2 shows the waveguide grating frequently treated as a benchmark [3], [16], [19], [21], in which the geometrical parameters are indicated. Due to the symmetry of the waveguide, only half the section ($x > 0$) is analyzed. For the TD-BPM, the input pulse ϕ_i is excited at $t = 0$, which consists of the eigenmode field ϕ_e in the x direction and the Gaussian profile with a $1/e$ half-width of 2 μm in the z direction, i.e.,

$$\phi_i(x, z, t=0) = \phi_e(x) \mathrm{e}^{-\left(\frac{z-z_0}{2}\right)^2} \mathrm{e}^{-j\beta(z-z_0)} \tag{16}$$

where β is the propagation constant of the eigenmode at the center wavelength and z_0 is the center position of the input pulse ($z_0 = 7$ μm). For the FDTD, the pulse is excited at z_0 using the one-way excitation scheme [2] (another excitation scheme can be employed [32], [33]). The perfectly matched layer (PML) [34]–[36] is utilized as an absorbing boundary condition (ABC).

Before comparing TD methods, we preliminarily investigate two treatments of modeling the waveguide grating. First, we calculate the grating by the WB-TD-BPM with the IFD2, taking into account an arbitrary position of the dielectric interface between the sampling points [22], [23], in which the grating structure is correctly modeled (for the FDTD, an arbitrary dielectric interface can also be modeled by a combination of the boundary condition and one-sided difference operator [37]–[39] or by an index averaging technique [40]). Next, we analyze the grating using the WB-TD-BPM under the assumption that each region in one grating period has the same length: $\Lambda_+ = \Lambda_- = 0.31895$ μm. In this case, one grating period can simply be divided by an integer. For both treatments, the dielectric interface can be analyzed with the second-order accuracy being maintained. As a result, we hardly find a distinct difference between the two numerical results, provided that the sampling width is small enough to yield a converged solution. Therefore, for simplicity, we adopt the latter treatment in the following analysis.

TABLE I
TD METHODS

Method	FDTD	SV-FDTD	FB-TD-BPM	WB-TD-BPM	NB-TD-BPM
Discretization Scheme in time	explicit	explicit	implicit Newmark-β ($\beta = 0.5$)	implicit 1) CN 2) CN + ADIM with iteration	implicit 1) CN 2) CN + ADIM
Solver	–	–	Bi-CGSTAB	Bi-CGSTAB for 1) Thomas for 2)	Bi-CGSTAB for 1) Thomas for 2)
ABC	PML [34]	PML [35]	PML [36]	PML [36]	PML [36]
Δt (femtosecond)	$\simeq 0.089$	$\simeq 0.089$	0.6	0.6 for 1), 1 for 2)	0.6 for 1), 1 for 2)

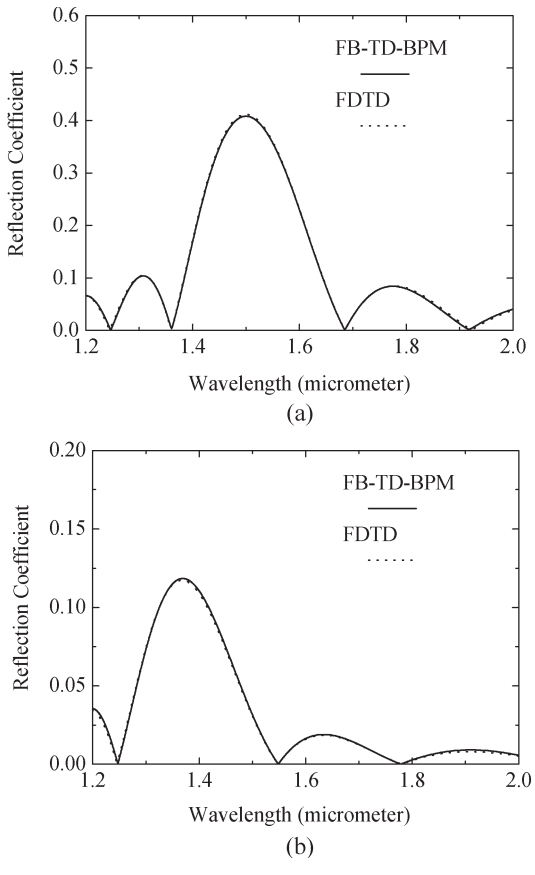

Fig. 3. Spectral response of the reflection coefficient for the FB-TD-BPM. (a) TE mode and (b) TM mode.

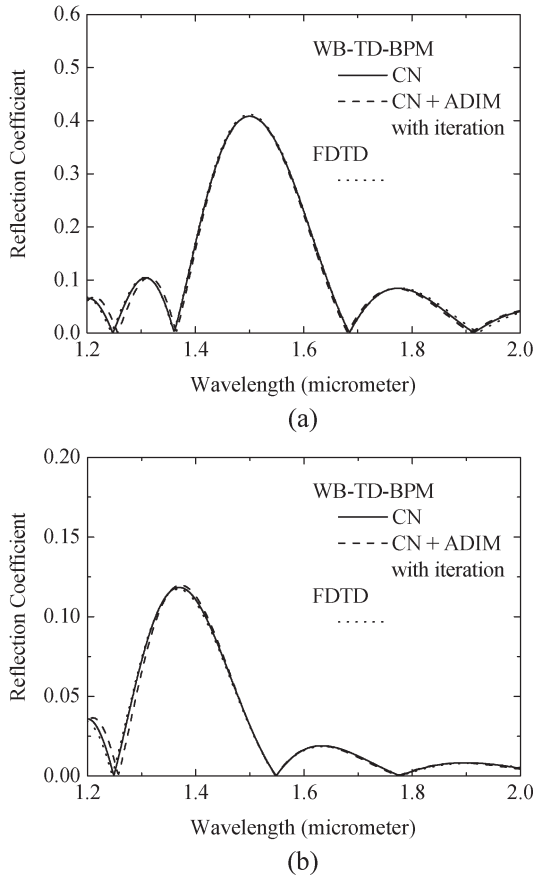

Fig. 4. Spectral response of the reflection coefficient for the WB-TD-BPM. (a) TE mode and (b) TM mode.

A. Comparison Among TD Methods With Second-Order Accuracy in Space

For each method listed in Table I, the second-order accuracy is achieved in space, even when the index discontinuity exists. To fairly compare the methods, we discretize the structure shown in Fig. 2 using the same spatial sampling widths: $\Delta x = 3.75 \times 10^{-2}$ μm and $\Delta z \simeq 3.99 \times 10^{-2}$ μm, in which the waveguide width and one grating period are divided by 8 and 16, respectively (preliminary calculations showed that the use of smaller Δx and Δz does not improve the accuracy of the numerical results). The number of sampling points is $N_x \times N_z = 74 \times 1110$, including 8 and 16 points used for the PML in the x and z directions, respectively.

The choice of the time step Δt is important for a TD method, because it predominates the amount of the computation. For the FDTD and SV-FDTD, Δt is taken to be $\simeq 0.089$ fs, which is slightly smaller than that determined by the stability criterion. For the TD-BPMs, taking advantage of the unconditional stability of the implicit scheme, we can choose a large Δt. However, we preliminarily find that when using the Bi-CGSTAB, a large Δt does not always contribute to a reduction in the computational time. This is because analyzing a large variation of the field, which results from a large Δt, may require a number of iterations to obtain a converged solution. Therefore, we choose a reasonably small Δt in such a way that the total computational time becomes nearly minimal (the residual in norm is set to be 10^{-6}). For the WB- and NB-TD-BPMs with the ADIM, we use the largest Δt that enables to yield a converged solution of the reflection coefficient. In Table I, Δt used for each method is summarized. The total

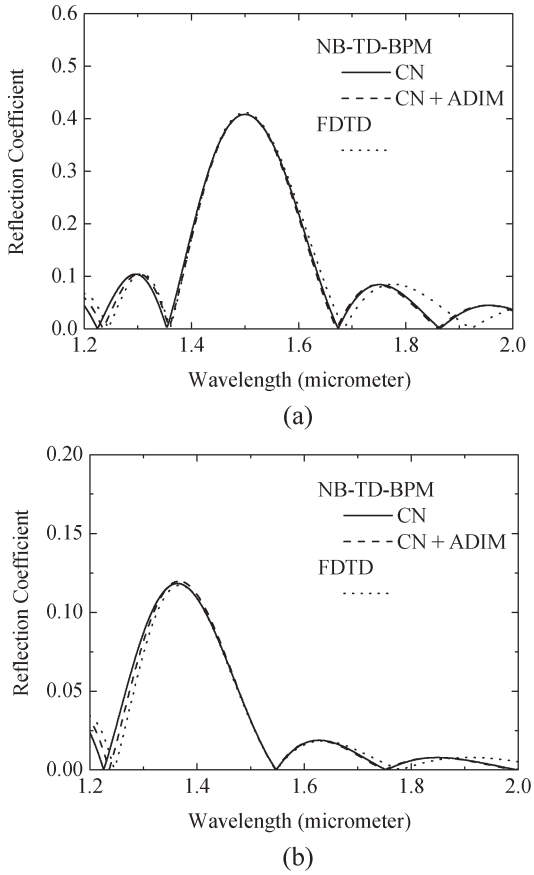

Fig. 5. Spectral response of the reflection coefficient for the NB-TD-BPM. (a) TE mode and (b) TM mode.

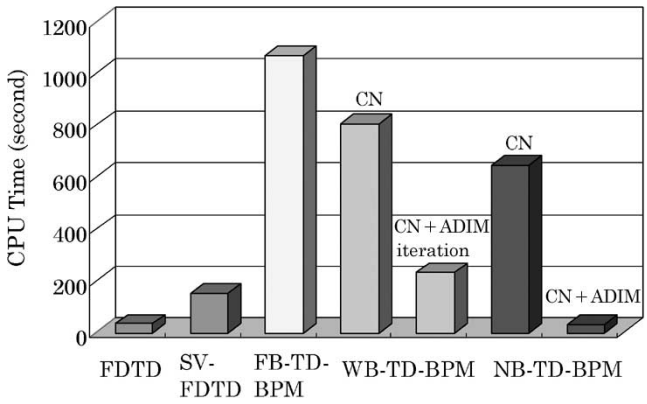

Fig. 6. CPU time for the TE mode analysis.

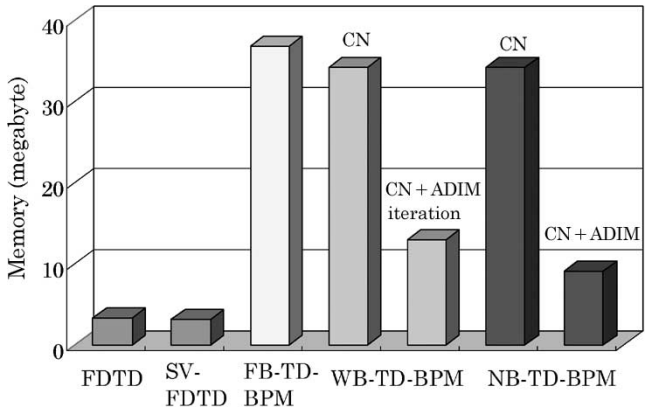

Fig. 7. Memory required for the TE mode analysis.

computational duration is 210 fs for the TE mode and 170 fs for the TM mode.

Figs. 3–5 show the spectral responses of the reflection coefficients calculated from the FB, WB, and NB-TD-BPMs, respectively, in which the center wavelength is fixed to be 1.5 μm for both TE and TM modes. The coefficient is evaluated from the ratio between the discrete Fourier transforms of the reflected pulse and the incident one observed at the reference plane depicted in Fig. 2. In these figures, also included for reference are the responses obtained from the FDTD. Although not illustrated, the responses from the SV-FDTD are in perfect agreement with those from the FDTD.

It can be found in Figs. 3 and 4 that the responses obtained from the FB- and WB-TD-BPMs agree quite well with those obtained from the FDTD. For the NB-TD-BPM in Fig. 5, the responses are in good agreement with those from the FDTD around the center wavelength (1.4–1.6 μm), although they deviate from those of the FDTD at wavelengths away from the center wavelength. This deviation is attributed to the omission of the temporal second derivative based on the SVEA. For the WB- and NB-TD-BPMs, the responses with the ADIM exhibit slight spectral shifts from those without the ADIM at a short wavelength.

It is interesting to note that for the WB-TD-BPM, the range where the deviation in the phase velocity is kept within $\pm 1\%$ in Fig. 1 covers a spectral range of 1.2–2.0 μm in Fig. 4. In addition, for the NB-TD-BPM, the corresponding range fairly agrees with a spectral range of 1.4–1.6 μm in Fig. 5. Remember that in these spectral ranges, the responses obtained from the TD-BPMs agree well with that from the FDTD. In general, it is not easy to predict optimum temporal and spatial sampling widths in advance, because they depend on the pulse width and the model to be analyzed. Roughly speaking, however, temporal and spatial sampling widths should be chosen so as to keep the error in the normalized numerical phase velocity within $\pm 1\%$, in order to obtain an accurate spectral response.

In Fig. 6, the CPU time required for the TE-mode analysis is presented. We use a PC with a Pentium 4 processor (2.26 GHz). The CPU time of the SV-FDTD is estimated to be longer than that of the FDTD. This is because the PML based on a three-step algorithm for the SV-FDTD [35] is computationally intensive. It is noteworthy that the use of the ADIM contributes to a reduction in the CPU time. In particular, for the NB-TD-BPM with the ADIM, the CPU time is slightly less than that of the FDTD. It is clear that the FB-, WB-, and NB-TD-BPMs without the ADIM are time consuming due to the solution of broadly banded matrices.

The computational efficiency is also checked in terms of the memory requirement for the TE mode in Fig. 7. Although the memory required for the SV-FDTD should be reduced when

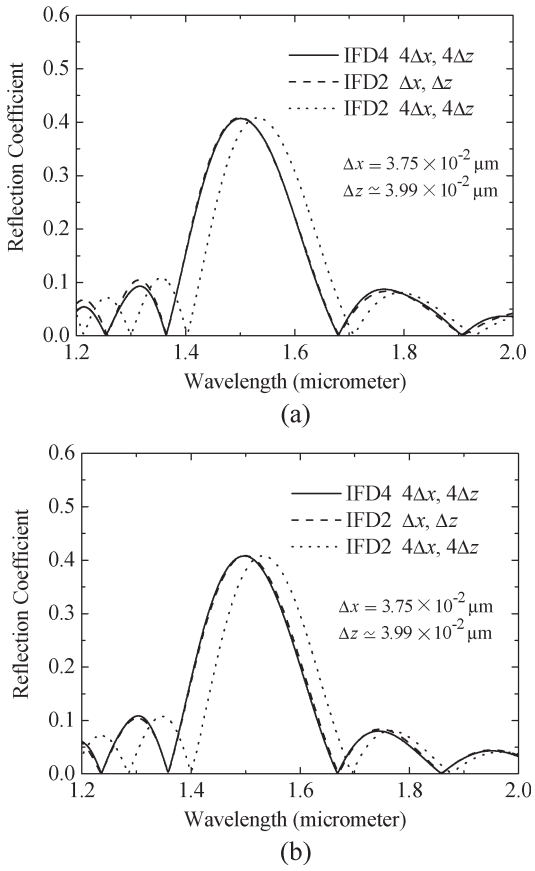

Fig. 8. Spectral response of the reflection coefficient. (a) WB-TD-BPM and (b) NB-TD-BPM.

compared with the FDTD, it is almost the same as that of the FDTD. This is due to the fact that the three-step PML algorithm for the SV-FDTD requires an extra memory. It is also seen that the implicit schemes, particularly when using the Bi-CGSTAB, require more memory than the explicit schemes.

B. Application of Fourth-Order Accurate FD Formula to ADIM-Based TD-BPMs

Final consideration is given to a further reduction in the CPU time of the ADIM-based TD-BPMs. We adopt the improved FD formula with fourth-order accuracy (IFD4) [41], which allows us to use a large spatial sampling width. The application of the IFD4 to the ADIM-based TD-BPMs has the advantage that the fourth-order accuracy is obtainable with a tridiagonal matrix being maintained, even when the index discontinuity exists [42]. The IFD4 has already been applied to the NB-TD-BPM [15]. We here develop a WB-TD-BPM based on the IFD4 and present the numerical results.

For the FDTD, the fourth-order accurate FD scheme is used to reduce the phase error of a propagating wave [43], [44]. However, as far as we know, there is no application of the higher order FD scheme considering the boundary condition at a dielectric interface to the FDTD (although the second-order FDTD has been developed for an arbitrary dielectric interface [37]–[39], the corresponding fourth-order FDTD has not yet been developed). Therefore, we do not investigate FDTDs based on the higher order scheme.

Fig. 8(a) and (b) shows the spectral responses for the TE mode obtained from the IFD4-based WB- and NB-TD-BPMs, respectively. For reference, also included are the responses obtained from the IFD2-based TD-BPMs discussed in Section IV-A. It can be found in Fig. 8 that the responses from the IFD4-based TD-BPMs (solid line) are in excellent agreement with those from the IFD2-based TD-BPMs (broken line), even when the spatial sampling widths are four times as large as those used in the IFD2. In contrast, when using the large widths, the responses from the IFD2-based TD-BPMs shift rightwards (dotted line). Although not illustrated, the IFD4-based TD-BPMs work well for the TM mode, as in the case of the TE mode.

It should be noted in the above case that the number of sampling points is reduced to $N_x \times N_z = 18 \times 277$, which leads to a substantial reduction in the CPU time. As a result, for the WB-TD-BPM, the CPU time is reduced to 40% of that of the FDTD, in which the spectral responses comparable to those of the FDTD can be obtained. Besides, the NB-TD-BPM yields the reduced CPU time to only 6% of that of the FDTD, while offering a close correspondence to the responses of the FDTD around the center wavelength (1.4–1.6 μm) which may cover the so-called *S*-, *C*-, and *L*-bands in optical communications.

V. Conclusion

We have compared several time-domain (TD) methods such as finite-difference time-domain (FDTD), scalar or semivector finite-difference time-domain (SV-FDTD), full-band time-domain beam-propagation method (FB-TD-BPM), wide-band time-domain beam-propagation method (WB-TD-BPM), and narrow-band time-domain beam-propagation method (NB-TD-BPM). After presenting the formulation, we perform the numerical dispersion analysis for each method. To assess the methods, we calculate the reflection coefficient of a waveguide grating. Although the numerical results of the FB- and WB-TD-BPMs agree well with that of the FDTD, the CPU times are longer than that of the FDTD due to the solution of broadly banded matrices. Introducing the alternating-direction implicit method (ADIM) significantly contributes to a reduction in the CPU time of the TD-BPM. Application of a highly accurate FD formula to the ADIM-based TD-BPM is effective in reducing the total number of sampling points, leading to a substantial reduction in the CPU time.

Acknowledgment

The authors would like to thank Dr. Y. Y. Lu of the City University of Hong Kong for invaluable discussions regarding time-domain methods.

REFERENCES

[1] A. Taflove and S. C. Hagness, *Computational Electrodynamics: The Finite-Difference Time-Domain Method*. Norwood, MA: Artech House, 2000.

[2] S. T. Chu, W. P. Huang, and S. K. Chaudhuri, "Simulation and analysis of waveguide based optical integrated circuits," *Comput. Phys. Commun.*, vol. 68, no. 1–3, pp. 451–484, Nov. 1991.

[3] W. P. Huang, S. T. Chu, A. Goss, and S. K. Chaudhuri, "A scalar finite-difference time-domain approach to guided-wave optics," *IEEE Photon. Technol. Lett.*, vol. 3, no. 6, pp. 524–526, Sep. 1991.

[4] W. P. Huang, S. T. Chu, and S. K. Chaudhuri, "A semivectorial finite-difference time-domain method," *IEEE Photon. Technol. Lett.*, vol. 3, no. 9, pp. 803–806, Sep. 1991.

[5] C. Conti, A. Di Falco, and G. Assanto, "Parametric oscillations in photonic crystal slabs 3-D time-domain analysis," *IEEE Photon. Technol. Lett.*, vol. 16, no. 6, pp. 1495–1497, Jun. 2004.

[6] T. Matsumoto and T. Baba, "Photonic crystal k-vector superprism," *J. Lightw. Technol.*, vol. 22, no. 3, pp. 917–922, Mar. 2004.

[7] Y. Ohtera, Y. Sasaki, and S. Kawakami, "Postprocessing of FDTD solutions for precise calculations of eigenfrequencies of photonic periodic structures utilizing the variational expression," *J. Lightw. Technol.*, vol. 22, no. 6, pp. 1628–1636, Jun. 2004.

[8] P. L. Liu, Q. Zhao, and F. S. Choa, "Slow-wave finite-difference beam propagation method," *IEEE Photon. Technol. Lett.*, vol. 7, no. 8, pp. 890–892, Aug. 1995.

[9] G. H. Jin, J. Harari, J. P. Vilcot, and D. Decoster, "An improved time domain beam propagation method for integrated optics components," *IEEE Photon. Technol. Lett.*, vol. 9, no. 3, pp. 348–350, Mar. 1997.

[10] F. Ma, "Slowly varying envelope simulation of optical waves in time domain with transparent and absorbing boundary conditions," *J. Lightw. Technol.*, vol. 15, no. 10, pp. 1974–1985, Oct. 1997.

[11] J. Shibayama, T. Takahashi, J. Yamauchi, and H. Nakano, "Finite-difference time-domain beam propagation method for analysis of three-dimensional optical waveguides," *Electron. Lett.*, vol. 35, no. 18, pp. 1548–1549, Sep. 1999.

[12] ——, "Time-domain finite-difference BPM with Padé approximants in time axis for analysis of circularly symmetric fields," *Electron. Lett.*, vol. 36, no. 4, pp. 319–321, Feb. 2000.

[13] ——, "Efficient time-domain finite-difference beam propagation methods for the analysis of slab and circularly symmetric waveguides," *J. Lightw. Technol.*, vol. 18, no. 3, pp. 437–442, Mar. 2000.

[14] ——, "Comparative study of absorbing boundary conditions for the time-domain beam propagation method," *IEEE Photon. Technol. Lett.*, vol. 13, no. 4, pp. 314–316, Apr. 2001.

[15] J. Shibayama, A. Yamahira, T. Mugita, J. Yamauchi, and H. Nakano, "A finite-difference time-domain beam-propagation method for TE- and TM-wave analyses," *J. Lightw. Technol.*, vol. 21, no. 7, pp. 1709–1715, Jul. 2003.

[16] M. Koshiba, Y. Tsuji, and M. Hikari, "Time-domain beam propagation method and its application to photonic crystal circuits," *J. Lightw. Technol.*, vol. 18, no. 1, pp. 102–110, Jan. 2000.

[17] J. J. Lim, T. M. Benson, E. C. Larkins, and P. Sewell, "Wideband finite-difference-time-domain beam propagation method," *Microw. Opt. Technol. Lett.*, vol. 34, no. 4, pp. 243–247, Jul. 2002.

[18] T. Fujisawa and M. Koshiba, "Time-domain beam propagation method for nonlinear optical propagation analysis and its application to photonic crystal circuits," *J. Lightw. Technol.*, vol. 22, no. 2, pp. 684–691, Feb. 2004.

[19] V. F. Rodriguez-Esquerre and H. E. Hernandez-Figueroa, "Novel time-domain step-by-step scheme for integrated optical applications," *IEEE Photon. Technol. Lett.*, vol. 13, no. 4, pp. 311–313, Apr. 2001.

[20] V. F. Rodriguez-Esquerre, M. Koshiba, and H. E. Hernandez-Figueroa, "Finite-element time-domain analysis of 2-D photonic crystal resonant cavities," *IEEE Photon. Technol. Lett.*, vol. 16, no. 3, pp. 816–818, Mar. 2004.

[21] S. S. A. Obayya, "Efficient finite-element-based time-domain beam propagation analysis of optical integrated circuits," *IEEE J. Quantum Electron.*, vol. 40, no. 5, pp. 591–595, May 2004.

[22] J. Yamauchi, M. Sekiguchi, O. Uchiyama, J. Shibayama, and H. Nakano, "Modified finite-difference formula for the analysis of semivectorial modes in step-index optical waveguides," *IEEE Photon. Technol. Lett.*, vol. 9, no. 7, pp. 961–963, Jul. 1997.

[23] J. Yamauchi, G. Takahashi, and H. Nakano, "Modified finite-difference formula for semivectorial H-field solutions of optical waveguides," *IEEE Photon. Technol. Lett.*, vol. 10, no. 8, pp. 1127–1129, Aug. 1998.

[24] N. M. Newmark, "A method of computation for structural dynamics," *J. Eng. Mech. Div., ASCE*, vol. 85, no. EM-3, pp. 67–94, Jul. 1959.

[25] H. A. Van Der Vorst, "Bi-CGSTAB: A fast and smoothly converging variant of Bi-CG for the solution of nonsymmetric linear system," *SIAM J. Sci. Stat. Comput.*, vol. 13, no. 2, pp. 631–644, Mar. 1992.

[26] D. W. Peaceman and H. H. Rachford, Jr., "The numerical solution of parabolic and elliptic differential equations," *J. Soc. Ind. Appl. Math.*, vol. 3, no. 1, pp. 28–41, Mar. 1955.

[27] J. Douglas, Jr. and H. H. Rachford, Jr., "On the numerical solution of the heat conduction problem in two and three variables," *Trans. Amer. Math. Soc.*, vol. 82, no. 2, pp. 421–439, Jul. 1956.

[28] H. Yokota, M. Hira, and S. Kurazono, "Iterative finite difference beam propagation method analysis of nonlinear optical waveguide excitation problem," *IEICE Trans.*, vol. J77-C-I, no. 10, pp. 529–535, Oct. 1994.

[29] H. Rao, R. Scarmozzino, and R. M. Osgood, Jr., "An improved ADI-FDTD method and its application to photonic simulations," *IEEE Photon. Technol. Lett.*, vol. 14, no. 4, pp. 477–479, Apr. 2002.

[30] Y. Y. Lu, "New unconditionally stable ADI schemes for the wave equation," presented at the 5th Pacific Rim Conf. Laser Electro-Optics, Taipei, Taiwan, 2003, W1A-(14)-2.

[31] N. N. Feng and W. P. Huang, "Time-domain reflective beam propagation method," *IEEE J. Quantum Electron.*, vol. 40, no. 6, pp. 778–783, Jun. 2004.

[32] J. B. Schneider, C. L. Wagner, and O. M. Ramahi, "Implementation of transparent sources in FDTD simulations," *IEEE Trans. Antennas Propag.*, vol. 46, no. 8, pp. 1159–1168, Aug. 1998.

[33] S. M. Wang, "On the current source implementation for the ADI-FDTD method," *IEEE Microw. Wireless Compon. Lett.*, vol. 14, no. 11, pp. 513–515, Nov. 2004.

[34] J. P. Berenger, "A perfectly matched layer for the absorption of electromagnetic waves," *J. Comput. Phys.*, vol. 114, no. 2, pp. 185–200, Oct. 1994.

[35] D. Zhou, W. P. Huang, C. L. Xu, D. G. Fang, and B. Chen, "The perfectly matched layer boundary condition for scalar finite-difference time-domain method," *IEEE Photon. Technol. Lett.*, vol. 13, no. 5, pp. 454–456, May 2001.

[36] C. M. Rappaport, "Perfectly matched absorbing boundary conditions based on anisotropic lossy mapping of space," *IEEE Microw. Guided Wave Lett.*, vol. 5, no. 3, pp. 90–92, Mar. 1995.

[37] K. H. Dridi, J. S. Hesthaven, and A. Ditkowski, "Staircase-free finite-difference time-domain formulation for general materials in complex geometries," *IEEE Trans. Antennas Propag.*, vol. 49, no. 5, pp. 749–756, May 2001.

[38] T. Ando, H. Nakayama, S. Numata, J. Yamauchi, and H. Nakano, "Eigenmode analysis of optical waveguides by a Yee-mesh-based imaginary-distance propagation method for an arbitrary dielectric interface," *J. Lightw. Technol.*, vol. 20, no. 8, pp. 1627–1634, Aug. 2002.

[39] C. P. Yu and H. C. Chang, "Yee-mesh-based finite difference eigenmode solver with PML absorbing boundary conditions for optical waveguides and photonic crystal fibers," *Opt. Express*, vol. 12, no. 25, pp. 6165–6177, Dec. 2004.

[40] G. Marrocco, M. Sabbadini, and F. Bardati, "FDTD improvement by dielectric subgrid resolution," *IEEE Trans. Microw. Theor. Tech.*, vol. 46, no. 12, pp. 2166–2169, Dec. 1998.

[41] Y. P. Chiou, Y. C. Chiang, and H. C. Chang, "Improved three-point formulas considering the interface conditions in the finite-difference analysis of step-index optical devices," *J. Lightw. Technol.*, vol. 18, no. 2, pp. 243–251, Feb. 2000.

[42] J. Yamauchi, T. Murata, and H. Nakano, "Semivectorial H-field analysis of rib waveguides by a modified beam-propagation method based on the generalized Douglas scheme," *Opt. Lett.*, vol. 25, no. 24, pp. 1771–1773, Dec. 2000.

[43] J. L. Young, D. Gaitonde, and J. S. Shang, "Toward the construction of a fourth-order difference scheme for transient EM wave simulation: Staggered grid approach," *IEEE Trans. Antennas Propag.*, vol. 45, no. 11, pp. 1573–1580, Nov. 1997.

[44] T. Hirono, W. W. Lui, K. Yokoyama, and S. Seki, "Stability and numerical dispersion of symplectic fourth-order time-domain schemes for optical field simulation," *J. Lightw. Technol.*, vol. 16, no. 10, pp. 1915–1920, Oct. 1998.

Jun Shibayama (M'03) was born in Kashiwa, Japan, on July 1, 1969. He received the B.E., M.E., and Dr.E. degrees from Hosei University, Tokyo, Japan, in 1993, 1995, and 2001, respectively.

In 1995, he joined Opto-Technology Laboratory, Furukawa Electric Company, Ltd., Ichihara, Chiba, Japan. Since 1999, he has been an Assistant at Hosei University. His research interests include numerical analysis of optical waveguides.

Dr. Shibayama is a Member of the Optical Society of America (OSA) and the Institute of Electronics, Information and Communication Engineers (IEICE) of Japan.

Mitsunori Muraki was born in Saitama, Japan, on April 5, 1981. He received the B.E. degree from Hosei University, Tokyo, Japan, in 2004 and is currently working toward the M.E. degree at the same University.

Mr. Muraki is a Member of the Institute of Electronics, Information and Communication Engineers (IEICE) of Japan.

Junji Yamauchi (M'85) was born in Nagoya, Japan, on August 23, 1953. He received the B.E., M.E., and Dr.E. degrees from Hosei University, Tokyo, Japan, in 1976, 1978, and 1982, respectively.

From 1984 to 1988, he served as a Lecturer in the Electrical Engineering Department of the Tokyo Metropolitan Technical College. Since 1988, he has been a member of the faculty of Hosei University, where he is now a Professor of Electronic Informatics. His research interests include optical waveguides and circularly polarized antennas. He is the author of *Propagating Beam Analysis of Optical Waveguides* (Baldock, Hertfordshire, U.K.: Research Studies Press, 2003).

Dr. Yamauchi is a Member of the Optical Society of America (OSA) and the Institute of Electronics, Information and Communication Engineers (IEICE) of Japan.

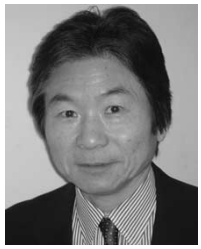

Hisamatsu Nakano (M'75–SM'87–F'92) was born in Ibaraki, Japan, on April 13, 1945. He received the B.E., M.E., and Dr.E. degrees in electrical engineering from Hosei University, Tokyo, Japan, in 1968, 1970, and 1974, respectively.

Since 1973, he has been a member of the faculty of Hosei University, where he is now a Professor of Electronic Informatics. His research topics include numerical methods for low- and high-frequency antennas and optical waveguides. He is the author of several books and many published articles.

Dr. Nakano received the IEE International Conference on Antennas and Propagation Best Paper Award and the IEEE TRANSACTIONS ON ANTENNAS AND PROPAGATION Best Application Paper Award (H. A. Wheeler Award) in 1989 and 1994, respectively. In 1992, he was elected an IEEE Fellow for contributions to the design of spiral and helical antennas. In 2001, he received the Award of Distinguished Technical Communication (from the Society for Technical Communication, USA) and the Science and Technology Progress Award (from Hangzhou, China). Prof. Nakano is an Associate Editor of several journals and magazines, such as *Electromagnetics*, IEEE ANTENNAS AND PROPAGATION MAGAZINE, IEEE ANTENNAS AND WIRELESS PROPAGATION LETTERS, and *Asian Information–Science–Life*.